May 2014

Northern Hemisphere Sea Level Pressure Synchronization and Its Effect on Northern Hemisphere Temperature Variability

Joshua Daniel Verbeten
University of Wisconsin-Milwaukee

NORTHERN HEMISPHERE SEA LEVEL PRESSURE SYNCHRONIZATION AND ITS EFFECT ON NORTHERN HEMISPHERE TEMPERATURE VARIABILITY

by

Joshua D. Verbeten

A Thesis Submitted in

Partial Fulfillment of the

Requirements for the Degree of

Master of Science

in Mathematics

at

The University of Wisconsin – Milwaukee

May 2014

ABSTRACT

NORTHERN HEMISPHERE SEA LEVEL PRESSURE SYNCHRONIZATION AND ITS EFFECT ON NORTHERN HEMISPHERE TEMPERATURE VARIABILITY

by

Joshua D. Verbeten

The University of Wisconsin – Milwaukee, 2014
Under the Supervision of Dr. Kyle Swanson

We consider monthly anomalies of zonally averaged sea level pressure (SLP) in the Northern Hemisphere (NH) from two reanalysis products. A measure of synchronization utilizing correlation coefficient in a five-year sliding window across all latitude pairs is computed over this data. It is found that there have been two NH SLP synchronization episodes since the 1890s, which are significant to approximately three standard deviations. Similar statistically significant synchronization events are seen in simulations of 42 global climate models (GCM) with the dominant synchronization pattern in GCMs proving dynamically consistent with observations. Furthermore, a GCM-based NH temperature anomaly composite shows a flattening of temperature time series in a decade prior to the synchronization episodes, a brief warming trend just after episodes, and a cooling trend thereafter, all of which agrees with the temperature structure around the observed synchronization episode seen in the 1890s. NH sea ice concentration anomalies are also composited from global climate models and show a decrease in ice concentration approximately one to two years after the maximum increase in temperature and an increase in ice concentration one to two years after the maximum

decrease in temperature. These results have substantial implications for climate prediction up to a decade in advance.

TABLE OF CONTENTS

LIST OF FIGURES

ACKNOWLEDGEMENTS

First and foremost, I would like to thank my mother and father for their continuous support throughout my academic career. I owe my deepest gratitude to Dr. Kyle Swanson for guiding me through this research experience, and to Dr. Sergey Kravtsov for his help with statistical analysis.

1 Introduction

In a pioneering work, *Tsonis et al.* (2007) showed that an important precursor of major climate shifts in large-scale climate patterns is short-term synchronization of climate variability across a wide range of its indicators. Under the right conditions, the synchronization is destroyed and a new climate state emerges. Therefore, they showed that it is important to document and characterize climate change surrounding observed, as well as simulated synchronization episodes.

In this study, following *Tsonis et al.* (2007), we aimed to better understand the dynamics of Northern Hemisphere (NH) climate variability conditioned on synchronization episodes diagnosed in the zonally averaged sea level pressure (SLP) field. The SLP synchronizations are characterized by this field's anomalies at different latitudes and how they vary in sync. SLP was chosen for synchronization based on the field's impact to low frequency variability within sensible weather and temperature patterns. In this approach, it is revealed that when statistically significant synchronizations in NH SLP are experienced, a distinct temperature pattern in the NH can be predicted thereafter.

Section 2 provides the reader with the data and methods that are used in this paper. Section 3 gives the results of observed and modeled SLP synchronization and temperature structure around significant synchronization episodes. We then discuss avenues for future work and give a summary of this work in section 4.

2 Data and Methodology

2.1 Data

For this study, we chose to analyze monthly NCEP/NCAR Reanalysis 1 (Kalnay et al., 1996) and 21st Century Reanalysis V2 (Compo et at., 2011), 1000mb geopotential height (h1000) and SLP data which is provided by the NAA/OAR/ESYL PSD in Boulder, Colorado USA (available at http://www.esrl.noaa.gov/psd). These products are produced through data assimilation methods that involve the recovery of land surface, ship, rawinsonde, aircraft, satellite, and other data observations, which are filtered into a dynamical model. We considered wintertime (December - February) data covering the NH, on a 144 x 37, $2.5°$ resolution spatial grid with temporal range from 1948 – 2013 for the Reanalysis 1 product and 1871 – 2013 for the Reanalysis (V2) product. NH winter months are chosen because wintertime variability in the NH is stronger than that during other seasons (Holton 1992), and hence, signal detection is easier. The data is then zonally averaged with the seasonal cycle removed to give the final monthly NH SLP anomaly dataset.

In addition, we also looked at observed NH surface temperature anomalies in this study. The dataset chosen for this field is the HadCRUT4 dataset, (Brohan et al. 2006), which takes surface temperature and sea surface temperature from 4,800 stations, which are separately averaged into a $5°$ resolution grid and then weighted (Morice et al. 2012) by latitude. The time series resulting from this dataset gives a good approximation of NH temperature anomaly evolution from 1850-2013.

In addition to observed data, we also considered Monthly Coupled Model Intercomparison Project version 5 (CMIP5) representative concentration pathway (RCP)

4.5 scenario model simulations of SLP and surface temperature. These fields were analyzed in a similar fashion as to the NCEP/NCAR Reanalysis product previously mentioned. The "4.5" is a midrange mitigation emissions scenario with temporal range extending from 1861–2100 (Taylor et al., 2012). A total of 42 individual contribution simulations are considered with zonally averaged NH SLP and NH temperature anomalies computed over a $2.5°$ resolution spatial grid.

In addition to the temperature and SLP fields from the CMIP5 RCP 4.5 climate models, NH sea ice concentration is also considered in this study. Unlike temperature and SLP, only nine model simulations of sea ice concentration from the CMIP5 RCP 4.5 climate models are made available to the public, once again with anomalies computed on a $2.5°$ spatial grid with the same temporal resolution.

2.2 **Synchronization Measure**

Following the work of *Tsonis et al.* (2007) we aimed to quantify how in sync NH SLP is at a given time, and thus; a measure of synchronization is created for this study. The measure of synchronization was computed by summing the absolute values of correlation coefficients between SLP time series at different latitudes computed over a five-year sliding window, for all possible latitude pairs. In obtaining the above multiple correlation coefficient, we used a weighted summation, in which the single correlation coefficient representing a given pair of latitudes was multiplied by the square root of the product of the cosines of these latitudes. The resulting multiple correlation coefficient is divided by the sum of all such square roots for normalization (so that the resulting multiple correlation coefficient is between 0 and 1). This weighting provides an area-

weighted synchronization measure. The resulting value of synchronization measure (or multiple correlation coefficient) was then assigned to the midpoint of the five-year window considered. The five-year window is then shifted ahead one time step with the same calculation performed until the end of the record is achieved.

3 Results

3.1 Observed SLP Synchronization

To filter out unpredictable white noise, we first subjected the zonally averaged NH SLP anomaly dataset from the Reanalysis 1 product to data compression via singular value decomposition

(1) $\mathbf{SLP} = \mathbf{X} \bullet \mathbf{V}$

where $\mathbf{X}$ represents the matrix of principle components (PCs) of the SLP dataset and the columns of $\mathbf{V}$ are the corresponding Empirical Orthogonal Functions (EOFs). With the first four terms of the decomposition (1) accounting for 98.6% of the total SLP variance, the remainder of the EOFs were discarded in the following analysis using the synchronization algorithm described in section 2.2.

The time series of synchronization measure from this analysis is plotted in blue, in Figure 1. For completeness, h1000 data is also synchronized (not shown), however, it is noted that the NH h1000 synchronization measure time series and NH SLP synchronization measure time series are approximately equal. Four local maximums of synchronization measure are seen in Figure 1, with an event in the early 1950s, an event in the early 1970s, an event in the late 1970s, and the most significant of the four events occurring in mid to late 2000s. Figure 1 also shows the mean (black line) and one

standard deviation of this synchronization time series (dashed black line). The peak in the synchronization measure of NH SLP in the mid to late 2000s takes a standard score of 3.13, where the standard score quantifies how many standard deviations a data point in a time series is away from the mean of the time series.

3.2 **Significance Testing Using Linear Inverse Modeling**

A stochastic linear inverse model (LIM) is utilized to determine whether or not the observed SLP synchronization peak in the mid to late 2000s is likely to be caused by intrinsic variability of the SLP system, or, otherwise, if it was forced externally. Linear inverse modeling is a data modeling technique, which fits a parametric multivariate red-noise model

(2) $\mathbf{X}^{n+1} - \mathbf{X}^{n} = \mathbf{B} \bullet \mathbf{X}^{n} + \mathbf{R}$

to the observed multivariate time series $\mathbf{X}$ by finding the set of coefficients $\mathbf{B}$ to minimize the difference between the left-hand side and right-hand side of equation (2). This is achieved via multiple linear regression. After model construction, synthetic realizations of the variable $\mathbf{X}$ time series can be obtained by simulating its evolution according to model (2) forced by the white-noise surrogates sampled from a distribution with the same covariance structure as that of $\mathbf{R}$. Per our earlier discussion, we performed LIM modeling in the subspace of the four leading PCs of SLP and using equation (2), we generate 1,000 surrogate sets of these PCs. The full NH SLP anomaly datasets are reconstructed from these PCs using equation (1), with the observed EOFs $\mathbf{V}$.

The 1,000 full surrogate datasets obtained by the LIM are then subjected to the same synchronization algorithm as described in section 2.2. The 95th percentile of the maximum values (over the whole simulation period) of synchronization measure in each of the 1,000 datasets is the red line plotted in Figure 1. This line signifies that peaks of similar or greater magnitude to the synchronization peak seen in the mid to late 2000s are likely to happen within the scope of the record (i.e. there is a 5% chance that there will be a peak of similar magnitude to that of the red line at some time throughout the period). Since the entire synchronization measure time series is below the red line, we conclude that the mid to late 2000s peak in synchronization is not unlikely to have come about due to intrinsic variability within the SLP field and may have not been forced by an outside source (since our empirical SLP model (2) has no representation of the external forcing). The green line is the mean of the 95th percentile of all time series values, *for a given year*, throughout all 1,000-surrogate synchronization time series. This line shows that it is very unlikely to see a synchronization peak of similar magnitude to the mid to late 2000s peak at any random year selected in the period (i.e. there is a 5% chance to see an event similar in magnitude to the green line at any discrete time throughout the period).

In summary, SLP synchronization events, of similar magnitude to the episode in the mid to late 2000s, appear to arise due to intrinsic SLP variability and, by themselves, may be difficult to predict. We will see below, however, that once the synchronization episode has been observed, we may expect a predictable behavior over the following decade in important climate variables, such as, NH temperature and sea-ice concentration/extent.

3.3 **NH Temperature Behavior Around Synchronization Episodes**

Encouraged by finding a significant NH SLP synchronization event in the mid to late 2000s, we then looked at a SLP dataset that extends further into the past than the NCEP/NCAR Reanalysis 1 dataset. In particular, the 21st Century Reanalysis (V2) dataset, with temporal range from 1871-2013, was subjected to the same synchronization algorithm described in section 2.2. The top panel of Figure 2 shows NH SLP synchronization of this late 19th to early 21st century dataset analogous to Figure 1. From the figure, we now see two significant synchronization episodes. The first synchronization episode we point out is the episode seen in the NCEP/NCAR Reanalysis 1 product, which obtains a local maximum in the mid to late 2000s. We note that the peak the Reanalysis (V2) is slightly less pronounced than that identified in the Reanalysis 1 product. However, another local maximum in SLP synchronization seen in the V2 product, which comes in the mid 1890s, has a peak with similar magnitude to the peak in the mid to late 2000s.

Having a synchronization peak in the past, rather than on the edge of the available data record, provides us with a unique opportunity to examine if an SLP synchronization episode may have any influence on temperature anomalies in the NH. Figure 2 also shows the NH temperature anomaly, in $^{\circ}C$, from the HadCRUT4 dataset. An examination of this anomaly shows no significant increase or decrease in temperature anomaly prior to the 1890 NH SLP synchronization episode, followed by an anomalous local increase in temperature starting at approximately at 1899, and an anomalous local decrease in temperature after 1910.

When considering the mid 2000s synchronization peak, we also see that there is no significant increase or decrease in temperature anomaly prior to the synchronization episode, consistent with an early 20th-century behavior, but we cannot say what happens afterwards, since the temperature anomaly structure after the episode is not yet available. The results described above on the NH temperature behavior associated with SLP synchronization thus far are interesting, but are statistically suspect, given that we only have two synchronization episodes to compare temperature structure around. To check for robustness of this behavior and to boost statistical significance, we next look into whether global climate models can produce and further rationalize this type of behavior.

3.4 **Global Climate Model Analysis**

To determine if global climate models (GCMs) show similar temperature structures around synchronization episodes as seen in observations, an analysis of 42 CMIP5 RCP 4.5 GCMs was performed. Once again, our purpose here is check if GCMs are simulating NH SLP synchronization episodes with magnitude similar to observations to increase synchronization sample size, and if this is the case, to document the temperature anomaly structure around these episodes.

It is important to increase the SLP synchronization sample size to understand if the observed temperature structure before and after episodes can be expected when we observe a significant SLP synchronization episode going forward; this possibility provides a potential bridge to interannual-to-decadal climate predictability. The next task then is to subject the 42 CMIP5 RCP 4.5 model simulations of NH SLP anomaly to the synchronization algorithm described in section 2.2.

The NH SLP anomaly fields provided from the GCM simulations do produce synchronization episodes with similar and, in some instances, greater magnitude than what is seen in the Reanalysis 1 product (see Figure 3). In fact, a total of 51 synchronization episodes occurring at or above the maximum synchronization peak in the observed mid to late 2000s peak (0.7251) are seen in the GCMs simulations we analyzed. In Figure 3, we plot three examples of model-based synchronization time series, with one model producing no episodes, one model producing one episode, and one model producing many episodes. Since we do see the similar NH SLP synchronization episodes in the models as we do in observations, we next examined, what happens to NH temperature around the episodes in the GCMs and look for similarities to the temperature structure seen in observations (see Figure 2., bottom panel).

Shown in Figure 4 are the NH (Figure 4a) and Arctic region (Figure 4b) temperature anomaly composites over the 20-year period centered on each of the GCM simulated 51 synchronization events, along with uncertainty thresholds obtained via surrogate compositing over a random year in the models that produce synchronization episodes. For consistency with the 51 members that produced the actual composite, the latter re-sampling procedure considered the same number of synchronization episodes for each sample as that of the number of observed synchronization episodes from their respective GCMs. The 97.5^{th} and the 2.5^{th} confidence levels based on 1,000 surrogate composites are also shown in Figure 4a and Figure 4b (black lines).

There is strong similarity between these two figures, especially with regards to when a significant positive and negative temperature anomaly arises following the synchronization episodes. The first significant temperature increase in Figure 4a and

Figure 4b comes approximately three to four years after a NH SLP synchronization episode with the anomaly peaking at $0.06\,°C$ and $0.37\,°C$ respectively. A significant decrease in temperature anomaly is seen after this maximum increase in temperature with a minimum in temperature anomaly peaking at -0.062 $°C$ and -0.32 $°C$ respectively at approximately eight years after the episode. The temperature then seems to approach zero after maximum decrease in temperature anomaly suggesting a decadal temperature variation time scale after synchronization episodes.

With the significant increase and subsequent decrease in temperature seen in GCMs after synchronization, especially in the Arctic region, Arctic sea ice concentration is analyzed in a similar fashion to temperature. The composite that is seen in Figure 5 is composed of 21 synchronization episodes from nine different CMIP5 RCP 4.5 model simulations where a synchronization episode is chosen if the peak arises above a 0.7251 synchronization measure threshold. Figure 5 suggests that there is a significant decrease in sea ice concentration approximately five years after synchronization episodes and a significant increase in sea ice concentration approximately ten years after synchronization episodes.

When comparing the sea ice concentration composite (Figure 5) with the temperature composite (Figure 4b), one can see that the significant increase/decrease in temperature leads the significant decrease/increase in sea ice concentration by approximately two years. This result makes physical sense in two ways; first, it appears that the sea-ice behavior is forced by the NH temperature (that is, warming causes a decrease in concentration), and second, that this process takes a bit of time due to the sea-ice thermodynamic and possibly dynamic inertia (so we wouldn't expect to see an

immediate impact on sea-ice concentration at exactly the same time as we see changes in the temperature structure).

3.5 **Spatial Structure of SLP Synchronizations**

It is important to understand whether or not the 42 GCMs models are dynamically consistent with observations to conclude that the temperature structure found in the GCMs is significant and is likely to be seen following possible future synchronization episodes. The main question we explore here is whether or not the modeled SLP synchronization episodes represent the same phenomenon as observations do and whether the same physical processes are leading to synchronization events for both GCMs and observations. If the modeled synchronization episodes do physically represent the same processes that observations show, the argued temperature structure after synchronizations episodes can confidently be used as a predictor for decadal temperature variability after a synchronization episode is experienced.

To explain whether or not observations and GCMs are representing the same SLP patterns that are contributing the most to synchronization, a latitudinal distribution analysis was performed. In particular, we computed the singular value decomposition of the correlation matrix $\mathbf{C}$ for a multivariate SLP time series, $\mathbf{S}$, over a five-year period centered at the synchronization episodes (linear trend was removed prior to the analysis):

(3) $\mathbf{C} = \mathbf{U} \bullet \mathbf{S} \bullet \mathbf{V}$

here $\mathbf{U}$ and $\mathbf{V}$ are identical matrices of spatial weights, whose columns correspond to the spatial pattern that contributes the most to the multiple correlation coefficient related to our synchronization measure.

This leading synchronization pattern is plotted in Figure 6 for all significant synchronization episodes this study has considered (53 episodes). First, the plots tell us how correlated each latitude band is with one another, for example, if a latitude band takes a value of 0.2 and a different latitude band takes a value of 0.2 as well, these bands are said to be in perfect correlation. Secondly, the plots tell us which latitude bands are contributing the most to the synchronization measure (i.e. multiple correlation coefficient) and are found at which latitude the plots take maxima and minima. By this analysis, we can say that the latitude bands that contribute the most to the synchronization measure are $15-30°N$ and $60-80°N$, which also are the latitude bands that hold maximum anti-correlation between one another (since they correspond to the largest positive and negative weights, respectively).

All of the 53 episodes shown in Figure 6 exhibit similar latitudinal structure with the exception of one GCM episode. This means that the vast majority of GCMs examined in this study agree with observations in that they simulate synchronizations episodes with robust spatial patterns consistent with the observed pattern. Therefore, we can conclude that our significance testing with regards to temperature and sea ice concentration anomaly composites are in fact an extension to observations and that the composites give a true representation of temperature and sea ice concentration in the 10-year period before and after NH SLP synchronization episodes, thus giving way to a new framework for forecasting decadal NH temperature variability.

3.6 **Synchronization Episode Connection to AO Index**

Lastly, to investigate which SLP pattern dominants the synchronization episodes we looked into the possible relationship between AO index (Thompson and Wallace, 1998) and SLP synchronization described in this study. With the correlation coefficient of the first EOF mode of our SLP dataset and the AO index being 0.83, it is concluded that the leading EOF of our SLP dataset effectively represents the AO index. The leading EOF mode of our SLP dataset is plotted in Figure 6, in blue, and shows that it exhibits the same spatial pattern as the leading mode of synchronization episodes considered previously. This suggests that the trailing modes of our SLP dataset gives minimal contribution to the synchronization measure used in this study. To test if the first EOF mode of our SLP dataset (AO index) dominates our synchronization measure compared to trailing EOF modes, an AO-dominance ratio is created. This ratio goes as

$$(4)\quad Ratio = \frac{\sum \mathbf{X}_1^2}{\sum \mathbf{X}_{2-4}^2}$$

where $\mathbf{X}^2$ are the squared PCs of the SLP dataset, with subscripts indicating which modes are summed. This ratio is computed over a five-year sliding window over the 20th century reanalysis dataset and is plotted in Figure 7, in blue. The synchronization measure described in section 2.2 is also plotted in Figure 7, in green. From the figure, we see that there are local maximums in AO-dominance ratio where we see the two significant synchronization episodes (1890s and 2000s). These results lead us to believe that since the AO index exhibits similar spatial structure to synchronization episodes, and that the AO-dominance ratio takes maxima at synchronization episodes, we are likely to see

synchronization episodes when the trailing EOF modes interfere least with the leading (first) EOF mode (AO index).

4 Summary and Future Work

Zonally averaged NH SLP anomalies in observations and GCMs are shown to exhibit rare, but climatically important synchronization episodes during which the polar SLP becomes abnormally anti-correlated with tropical SLP. The two observed events occurred in the 1890s and then again in the mid to late 2000s. Significance testing using an empirical SLP model simulating its intrinsic variability shows that episodes are not unlikely to happen due to intrinsic variability and that they are essentially unpredictable by themselves. However, a look at temperature structure around these episodes provides a promise for predictability. In particular, the NH temperature anomaly shows no increase/decrease just prior to the synchronization event but an interannual oscillation afterwards, with a warming and then cooling trend in the 10-year period following the synchronization episodes. All of this behavior, including the existence of abnormal SLP synchronizations, the dominate latitudinal pattern of synchronization episodes, as well as the interannual temperature trends around the SLP synchronization, is shown to be ubiquitous and statistically significant in GCMs, thus providing a useful framework for climate prediction on interannual-to-decadal time scales.

There are many avenues to explore with regards to future work to pursue following the results presented in this study. First, it would be useful to build off of section 3.6 and dig deeper into how and why these synchronization episodes happen. Are the episodes exclusively being driven by intrinsic variability or are they forced somehow by

interacting climate modes or external forcing? Second, it would be worthwhile to look into other climate/weather related variables to see if they are also being affected around synchronization episodes, much like how temperature is.

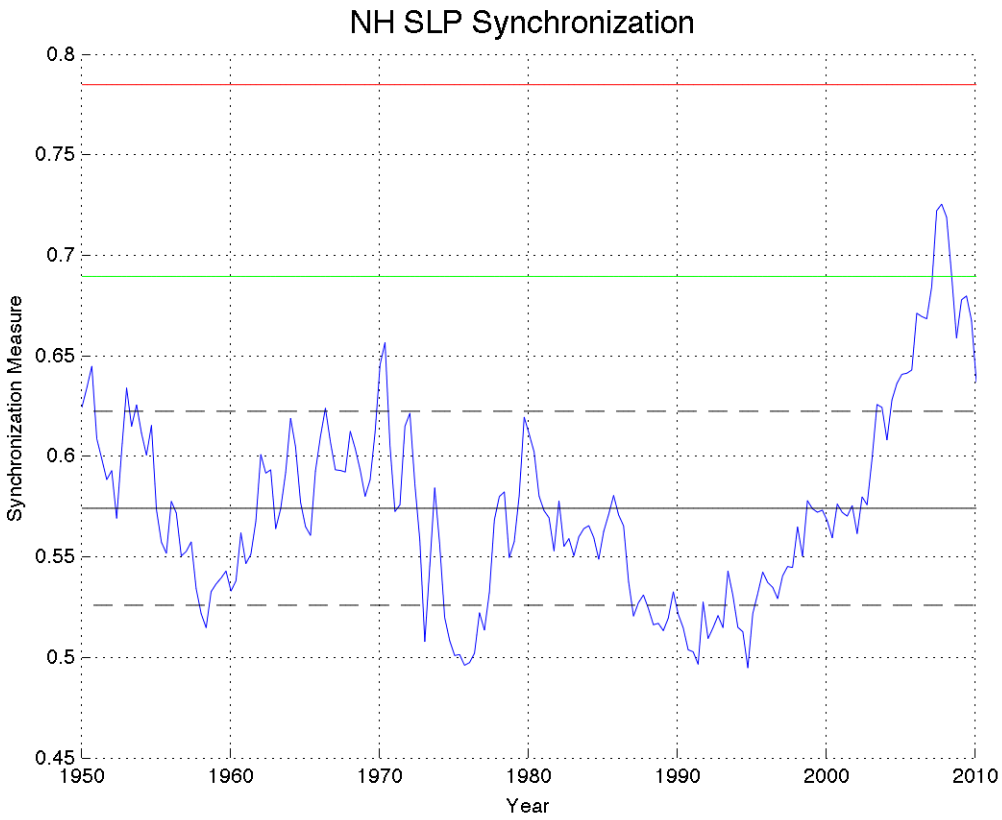

Figure 1. Synchronization measure time series taken from reconstructed NH SLP anomaly time series using four leading modes, in blue. Mean of this time series is plotted in solid black with one standard deviation plotted in dashed black. The chance of seeing a synchronization peak throughout the period here at the red line is 5%. The chance of seeing a synchronization peak at a discrete time at the green line is 5%.

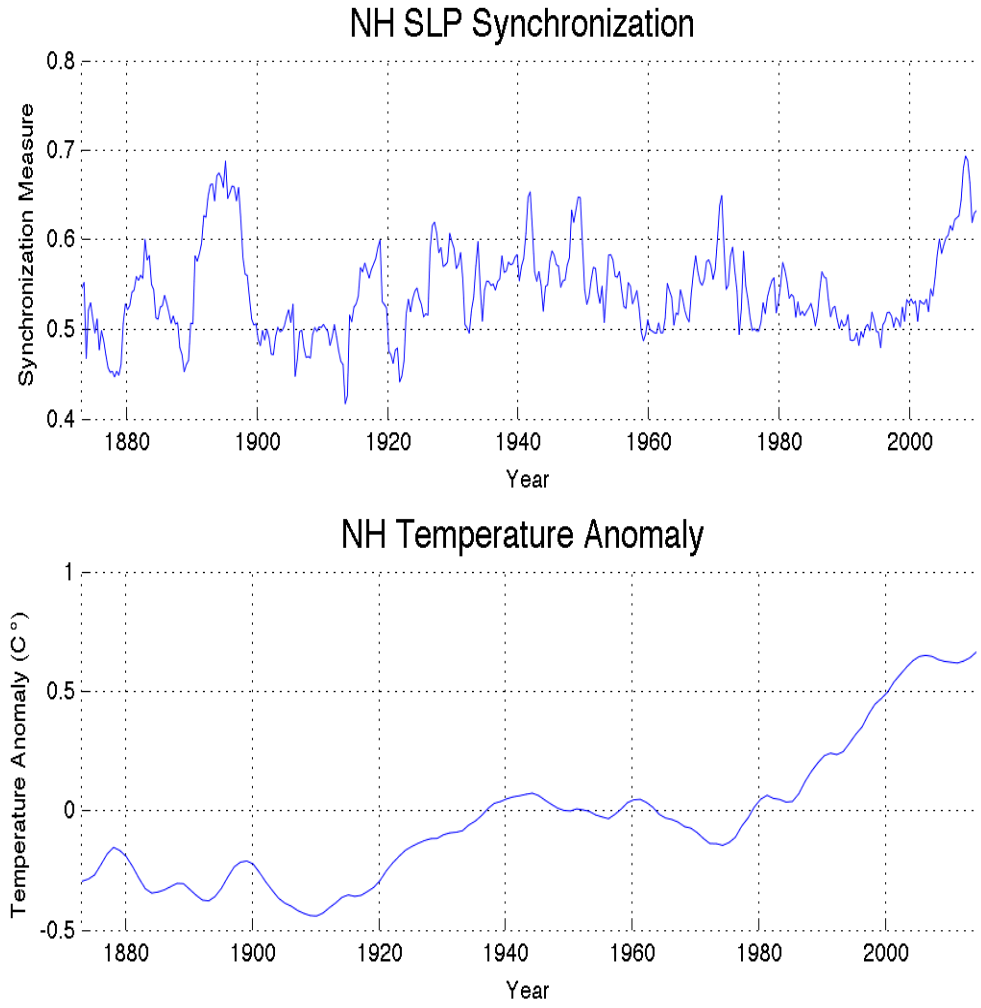

Figure 2. Top panel: NH SLP synchronization measure using 20th Century Reanalysis (V2) from 1873-2010. Bottom panel: HadCRUT4 NH temperature anomaly.

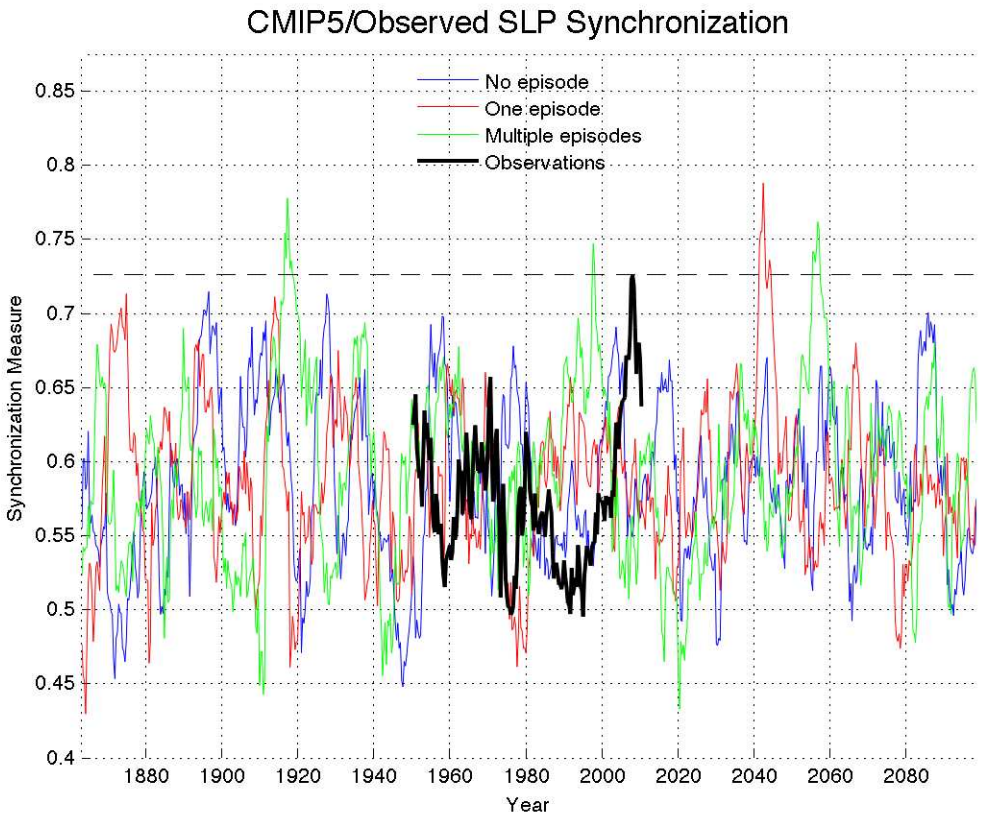

Figure 3. Three SLP synchronization measure time series from the CMIP5 RCP 4.5 GCMs. No significant synchronization episode in blue, one episode in red, multiple episodes in green, and observations in black. 95th percentile of all model synchronization time series is plotted in dashed black and is approximately the value of the significant episode peak seen in observations.

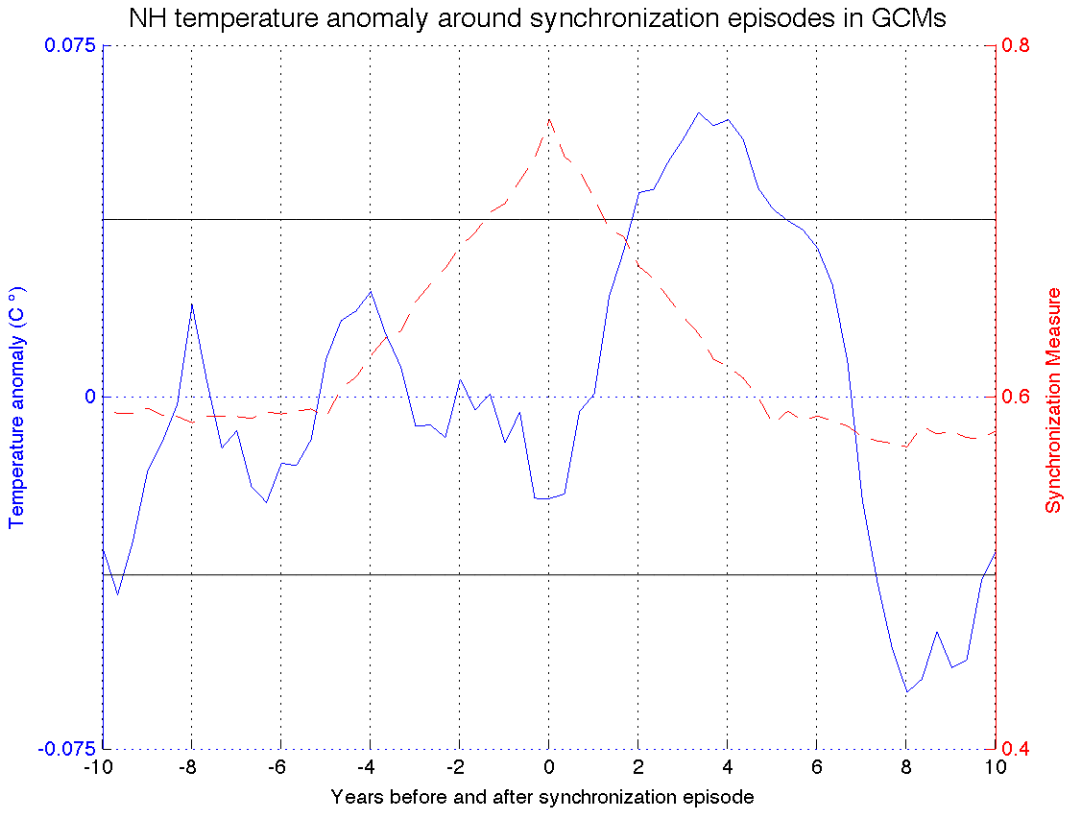

Figure 4a. NH temperature anomaly composite around 51 significant NH SLP synchronization episodes from 42 CMIP5 RCP 4.5 model simulations in blue. 97.5th and 2.5th significance levels from re-sampling in black. Composite of the 51 synchronization episodes plotted in dashed red.

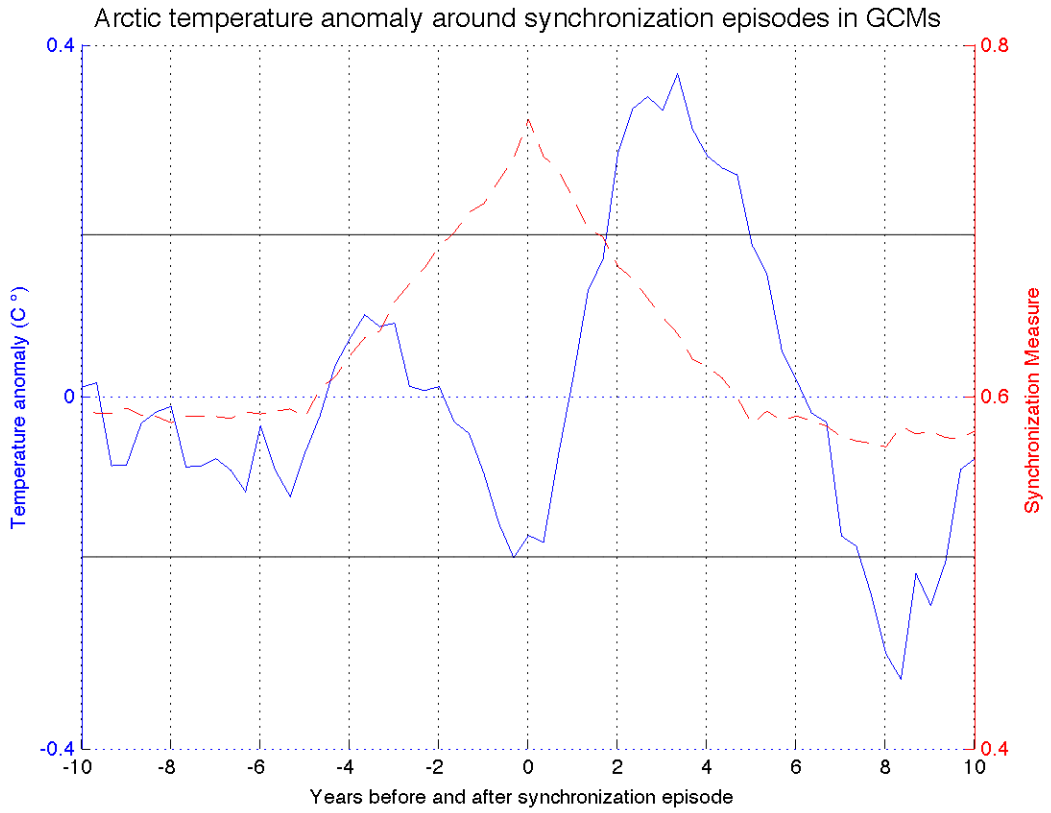

Figure 4b. Arctic region ($70-90°N$) temperature anomaly composite around 51 significant NH SLP synchronization episodes from 42 CMIP5 RCP 4.5 model simulations in blue. 97.5^{th} and 2.5^{th} significance levels from re-sampling in black. Composite of the 51 synchronization episodes plotted in dashed red.

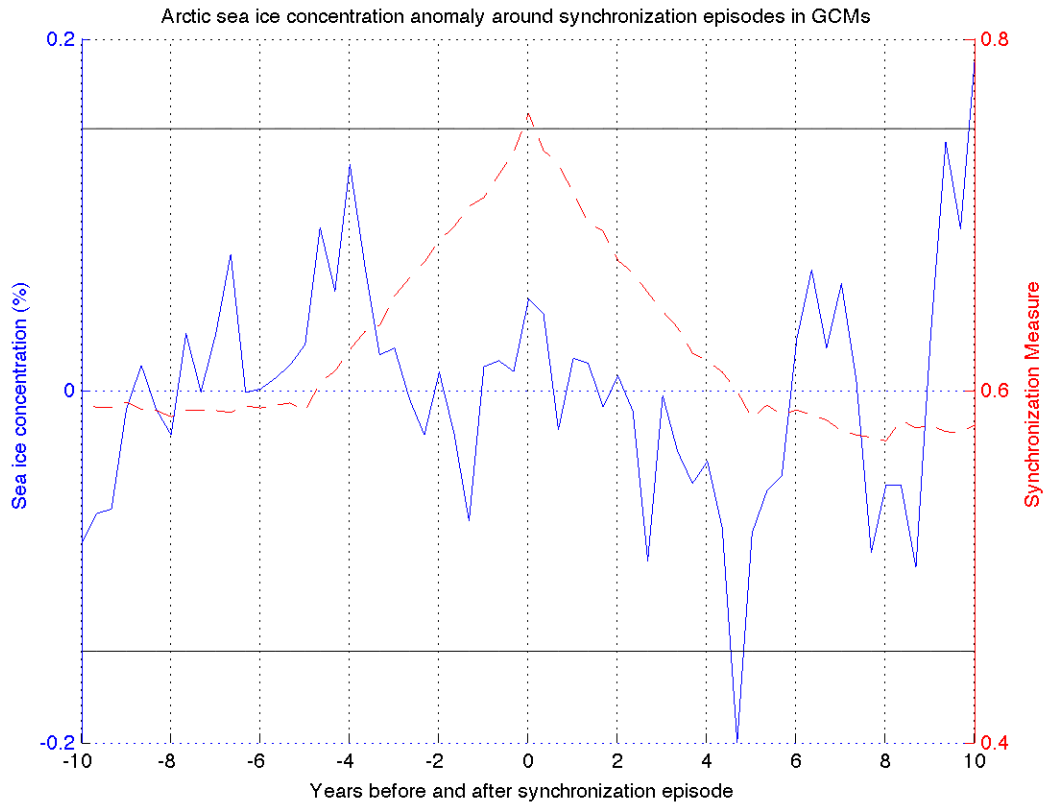

Figure 5. Arctic sea ice concentration anomaly composite around significant NH SLP synchronization episodes from 9 CMIP5 RCP 4.5 model simulations in blue. 97.5th and 2.5th significance levels from re-sampling in black. Composite of the 21 synchronization episodes plotted in dashed red.

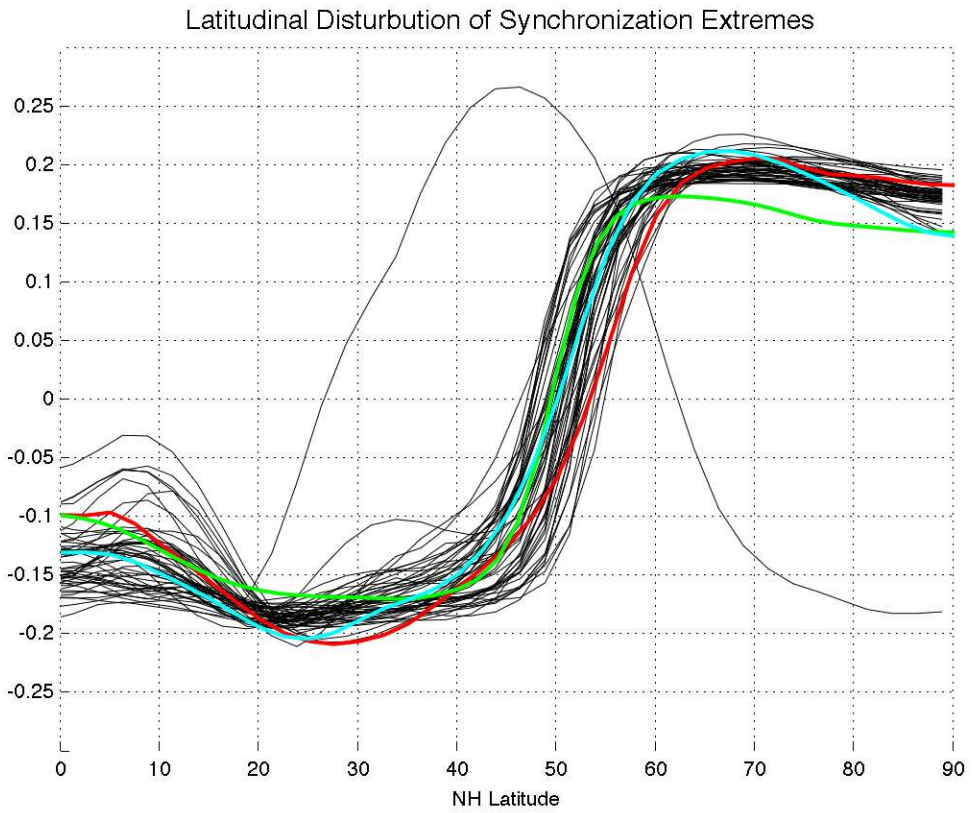

Figure 6. Latitudinal distribution analysis of 53 significant NH SLP synchronization episodes. 51 synchronization episodes seen in models in black. The 1890s synchronization episode seen in green and the mid to late 2000s episodes seen in red. The leading EOF mode (AO index) in light blue.

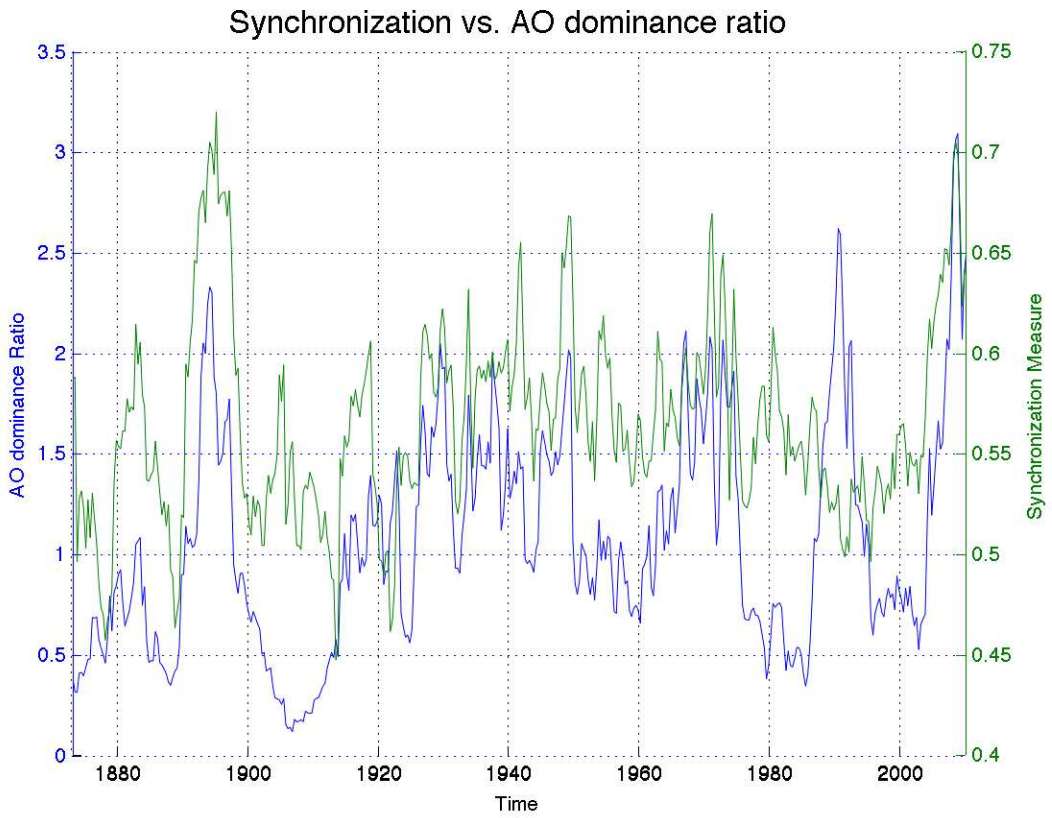

Figure 7. Synchronization measure from the 20th century reanalysis V2 dataset in green. AO dominance ratio as described in equation (4), in blue.

REFERENCES

Brohan, P., J.J. Kennedy, I. Harris, S.F.B. Tett and P.D. Jones, 2006: Uncertainty estimates in regional and global observed temperature changes: a new dataset from 1850. *J. Geophysical Research* **111**, D12106, doi:10.1029/2005JD006548

Compo, G. P. et al., The Twentieth Century Reanalysis Project. Q.J.R. Meteorol. Soc., 137: 1–28. doi: 10.1002/qj.776, 2011.

Holton, J. R., 1992: An Introduction to Dynamic Meteorology, 3d edition, Academic Press, p. 228-230.

Kalnay et al., The NCEP/NCAR 40-year reanalysis project, Bull. Amer. Meteor. Soc., 77, 437-470, 1996.

Morice, C. P. et al., Quantifying uncertainties in global and regional temperature change using an ensemble of observational estimates: The HadCRUT4 data set, J. Geophys. Res., 117, D08101, doi:10.1029/2011JD017187.

Taylor, Karl E., Ronald J. Stouffer, Gerald A. Meehl, 2012: An Overview of CMIP5 and the Experiment Design. *Bull. Amer. Meteor. Soc.*, **93**, 485–498.

Thompson, D. W. J. and J. M. Wallace: The Arctic Oscillation signature in the wintertime geopotential height and temperature fields. Geophys. Res. Lett. , 25 , 1297-1300. 1998.

Tsonis, A.A., Swanson, K. and Kravtsov, S. (2007). A new dynamical mechanism for major climate shifts. Geophysical Research Letters 34, L13705.